

Prediction of the stress-strain behaviour in rock by mechanical tunnel driving with tubbing segment support

Dipl.-Ing. Jürgen Schmitt, Prof. Dr.-Ing. Joachim Stahlmann

Institute of Foundation Engineering and Soil Mechanics, Technical University of Braunschweig

1 Introduction

The design of a mechanical tunnel driving in rock with tubbing segment support represents a special challenge for the engineer. Besides the estimation of the generally feasibility of this driving, the optimal selection of the design ground pressure for economical dimensioning is essential.

During the driving with a tunnel boring machine with a shield (TBM-S), temporary full section results from the cutting tools which is greater than the cross sectional area of the shield. This difference is labelled “overcut” (Fig. 1). When driving in rock the overcut avoids blocking the cutterhead and reduces the feed forces. To comply with the recommendations of the DAUB (DAUB 2005) the area of the shield skin should be dimensioned by the overcut and the shield conicity to ensure the shield machine is affected by load in solid rock as minimally as possible or to avoid it completely if at all feasible. So the determination of the planned overcut represents the necessary criterion for the feasibility of a project.

In practice the determination of the overcut will be defined by experience of realised projects. There is a lack of an analytical formulation to define the overcut, for example from the rock mechanics properties.

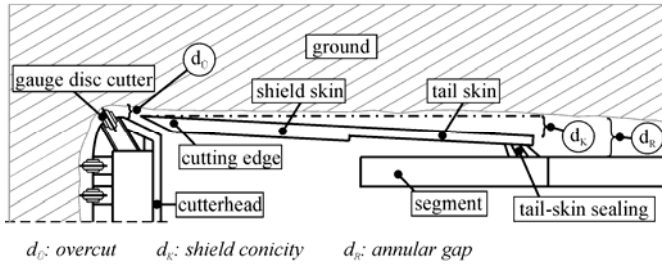


Fig. 1 Pattern sketch overcut, shield conicity, annular gap

In the design of the tubing segment support, the choice of the design ground pressure is important. The choice of the overburden pressure, as for mechanical tunnel driving in soft soil, will lead to an uneconomical tubing segment thickness, especially in tunnels with higher overburdens. Also, the stress-strain behaviour of the rock will be neglected by the bulk of established design ground pressures. A design ground pressure especially for a driving with a TBM-S is completely lacking.

2 Numerical calculations

For the analysis of the stress-strain behaviour of rock in mechanical driving with tubing segment support, extensive sensitivity with a three-dimensional numerical simulation model was carried out. For the three-dimensional numerical analyses, the program $FLAC^{3D}$ (Fast Lagrangian Analysis of Continua in 3-D) based on the finite difference method (FDM) was used.

2.1 Numerical model

In the calculation model the shield skin, tubing segment support, overcut and gap backfilling were generated (Fig. 2). The sideways edge distances and the lower edge distance of the geometric calculation model were defined according to the recommendations of the Research Group 1.6 “Numerik in der Geotechnik“ of DGGT (Meißner 1996). To generate an efficient calculation model, only the shield skin with the substitute thickness of the TBM-S was meshed. Also, the tubing segment was generated with a constant thickness without any tubing segment hinges. Following the recommendations of the DAUB (DAUB 2005) only in the area of the bottom of the TBM-S was a bedding considered.

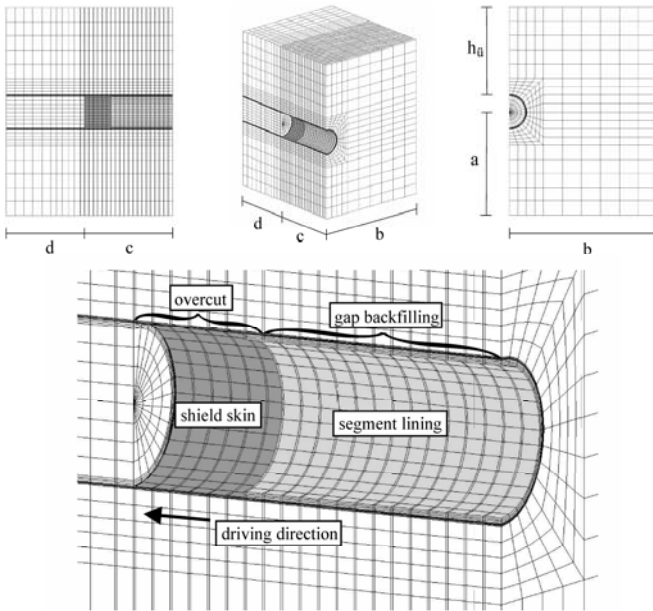


Fig. 2 Numerical model TBM-S

The material modelling of the shield skin, the tubing segment support and the gravel of the gap backfilling were simulated with linear elastic material behaviour and the material properties reported in Table 1. Because of the simplification in the geometric calculation model a conversion for the e-modulus and unit weight of the shield skin was executed. For the gravel of the gap backfilling a constant e-modulus was assumed.

Material properties	Unit	Shield skin (S235)	Segment lining (C35/45)	Gravel of gap backfilling
E-modulus / substitute e-modulus	[MN/m ²]	210,000/ 150,000*	33,500	100
Poisson's ratio	[-]	0.3	0.2	0.35
Unit weight / substitute unit weight	[kN/m ³]	75.0/ 615.0*	24.0	16.0

Table 1 Material properties of shield skin, segment lining and gravel of gap backfilling

The material behaviour of the rock was simulated with elastoplastic constitutive laws. On the one hand a constitutive law with linear elastic ideal plastic stress-strain behaviour and a Mohr-Coulomb failure criterion was used. On the other hand a constitutive law with an extension of the above mentioned constitutive law, the ubiquitous joint model, was used. This constitutive law permits the analysis of the influence of an interface on the stress-strain behaviour of the rock. A time-dependent stress-strain behaviour of the rock was not an element of the studies carried out.

The computations were performed as a step by step analysis. In addition, 20 load cases and/or states during construction were modelled. After the computation of the primary state of stress, the driving of the TBM-S was simulated. The state during construction #7 simulates the activated first ring of lining segments near the shield tail of the tunnel machine. State #8 activates the following ring of lining segments and replaces the material of the shield tail with the material of the gap backfilling.

The simulation of the contact pressure p_A at the working face was highly simplified with a steady distributed load, which was varied in the course of the sensitivity studies.

For the calculations a dry rock was assumed. Therefore mechanical loading from water pressure was not considered.

2.2 Sensitivity studies

The above described numerical model sensitivity studies were carried out to analyse the theoretical stress-strain behaviour of the rock.

In the sensitivity studies, in considering the isotropic material behaviour of the rock, the parameters of the rock, the overburden $h_{\text{ü}}$, the outer diameter of the tubing segment D_{TR} , the thickness of the tubing segment d_{T} , and the contact pressure p_A were varied. In Table 2 the individual parameters and the range within which they were varied are summarised. The range within the parameters for the rock were varied based on an extensive literature research. A possible tensile strength σ_t for the rock was not considered. The results of the analysis of the influence of an interface on the stress-strain behaviour of the rock with the ubiquitous joint model will not be described in this article.

Parameter	Unit	Range of parameters
Unit weight of rock mass γ	[kN/m ³]	17 to 26
E-modulus of rock mass E_{Gebirge}	[MN/m ²]	100 to 20,000
Poisson's ratio of rock mass μ	[-]	0.2 to 0.4
Angle of friction of rock mass ϕ_{Gebirge}	[°]	15 to 45
Cohesion of rock mass c_{Gebirge}	[MN/m ²]	0.1 to 2.0
Overburden $h_{\text{Ü}}$	[m]	30 to 1,000
Outer diameter segment lining D_{TR}	[m]	5.0 to 17.5
Thickness tubing segment d_{T}	[cm]	10 to 50
Contact pressure p_{A}	[kN/m ²]	0 to 1,000

Table 2 Range of parameters (isotropic properties of material)

3 Calculation results

Due to the amount of calculation results, an extensive presentation is not given in this article. Instead, several exemplary results are shown schematically and commented on. An extensive presentation of the calculation results is carried out elsewhere.

The maximum displacement after the generation of the overcut results in the area of the shield tail (section $U_{\text{I}}-U_{\text{I}}$, Fig. 3). With increases in the overburden $h_{\text{Ü}}$ the vertical displacement grows commensurately in the roof. All calculations show that the maximum vertical displacement can be found in the roof. Therefore the necessary criterion to estimate a blocking of the shield skin will be decided by the vertical displacement in the roof u_{Firste} .

The calculations show that the decisive influence on the value of the vertical displacement in the roof u_{Firste} results in the overburden, the e-modulus of the rock and also the shear strength of the rock (Table 3).

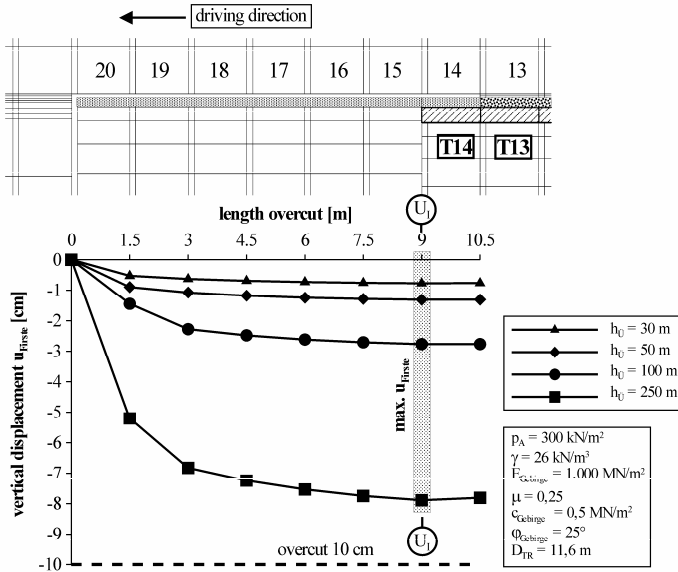


Fig. 3 Vertical displacement in the roof in the longitudinal section of the overcut

In Fig. 4 the deformation of the rock in the unsupported area generated by the overcut and associated stress rearrangement, which were calculated in the area of the full section in the roof and in the bottom, are displayed in a pattern sketch. This sketch shows the complexity of the stress rearrangement in several areas of the tunnel driving. When driving with a TBM-S, there is a rapid rise in the radial stresses at the cutter head after a distance of ca. 1.7 tunnel diameters, which increase greatly in the area of the working face. In the area of the overcut, no radial stresses result because of the missing support and consequent missing backpressure. After the installation of the segment lining in the shield tail and the gap backfilling the stresses in the roof increase. At a distance of ca. 1.6 tunnel diameters after the working face the stresses have a constant value. The radial stresses in the side wall of the tunnel not shown in Fig. 4 have qualitatively the same gradient as in the roof.

In the area of the bottom of the TBM-S the radial stresses decrease continuously until the stresses have a constant value after a distance of ca. 1.6 tunnel diameters. The self-weight of the TBM-S impacts in the area of the bottom (Fig. 4). This means that the calculated stresses in the bottom of the TBM-S of ca. 250 kN/m²

result from the self-weight of the TBM-S. This temporary loading is ineffective in the area of the tubing segment support and is the reason for the increase in radial stresses.

For the design of the tubing segment support, the ground pressure, which occurs at a distance of ca. 1.6 tunnel diameters after the working face, is decisive (Fig. 4).

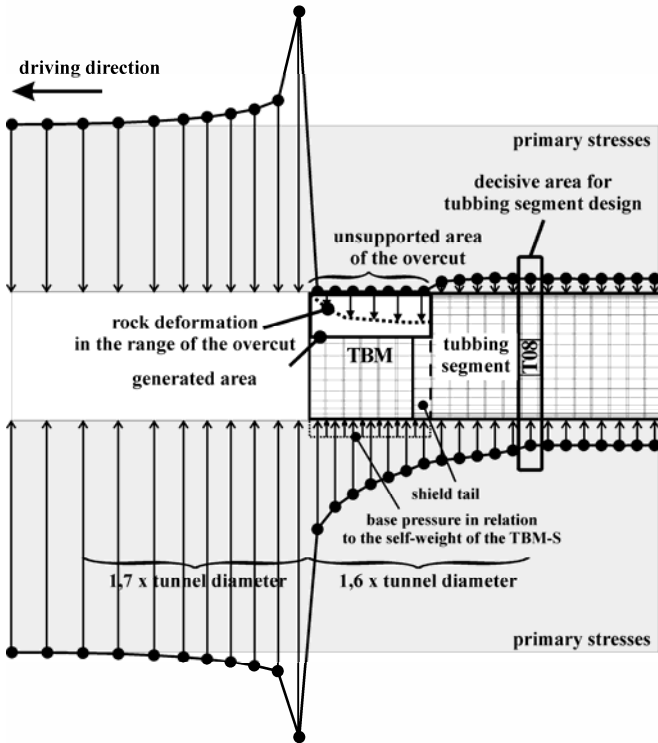


Fig. 4 Pattern sketch of the rock deformation in the overcut area and the stress rearrangement in the ground for a TBM-S

Figure 5 shows an example of a comparison between the calculated ground pressure within the sensitivity studies in the decisive area for the design of the tubing segment support (Fig. 5(b)) and the design loads in the design of the tubing segment support that are common in practice (Fig. 5(a)).

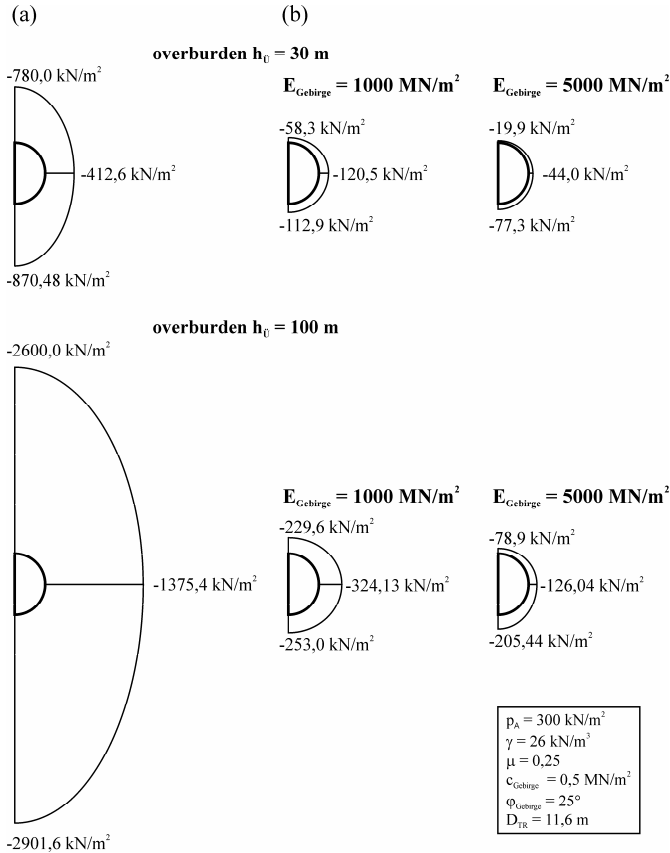


Fig 5 Comparison of (a) design loads according to DGEG (DGEG 1980) and (b) calculated ground pressure sensitivity studies

In practice, the design loads used are based on the recommendations of the DGEG (DGEG 1980), which refer to shield drivings in the loose rock. These recommendations are valid for tunnels with small to moderate depth situations. A definition of the term “moderate depth situation” is not given therein. However in the recommendations, statements are given regarding the concept of tunnels with an overburden which is larger than or equal to the three-way tunnel diameter. As in the highly simplified two-dimensional computation models described in the recommendations, a continuum ring with radial bedding is suggested, for example. The overburden pressure, which results from the product of the complete

overburden height and the density of the rock, is set as the load for these computation models.

In Fig. 5 it becomes impressively clear that these design loads are compared with the ground stresses for a mechanical tunnel driving determined in the sensitivity studies in the rock for a small overburden of $h_{\bar{U}} = 30$ m which are very conservative load assumptions. This difference increases a great deal with the rising overburden. Likewise it becomes unmistakably recognisable from the sensitivity studies accomplished that the mechanical material properties of the rock, for example the stiffness, have an influence on the size of the ground stresses which is not negligible (Fig. 5(b)). The sensitivity studies accomplished show very descriptively and clearly that a detailed analysis of the stress-strain behaviour of rock is urgently necessary for a mechanical tunnel driving with tubing segment support in particular, as is monitoring of future tunnel drivings, in order to achieve more realistic and economical calculation formulations.

Parameter	u_{Firste}	$\sigma_{r,F}$	$\sigma_{r,U}$	$\sigma_{r,S}$
Unit weight of rock mass γ	++	++	++	++
E-modulus of rock mass E_{Gebirge}	++	++	++	++
Poisson's ratio of rock mass μ	0	0	+	0
Angle of friction of rock mass φ_{Gebirge}	++	++	++	++
Cohesion of rock mass c_{Gebirge}	++	++	++	++
Overburden $h_{\bar{U}}$	++	++	++	++
Outer diameter of segment lining D_{TR}	0	0	++	0
Thickness of tubing segment d_{T}	-	++	+	++
Contact pressure p_{A}	0	0	0	0
++	Cat. 1: strong influence			
+	Cat. 2: weak influence			
0	Cat. 3: no influence			

Table 3 Rating influence parameters without consideration of interfaces

In Table 3 gives an overview of the influence of the different parameters varied in the sensitivity studies on the vertical displacement in the roof in the area of the overcut u_{Firste} , the radial stresses in the roof $\sigma_{r,F}$, the radial stress in the side wall $\sigma_{r,U}$ and the radial stresses in the bottom $\sigma_{r,S}$ within the determined range for the design of the tubing segment support arrangement.

4 Analytical design formulations

Based on the extensive calculation results of the sensitivity studies, through which several decisive material and geometrical parameters were determined, the development of analytical design formulations based on regression analyses took place. On the one hand a criterion was defined by which the risk of a blockage of the shield skin can be estimated and consequently the size of the necessary regular overcut can be calculated (Fig. 6(a), Equations (1) - (7), Table 4). On the other hand, design formulations for the radial stresses of the ground for the rule showed that if the overcut range is sufficient over the entire shield skin length, to the design of the tubing segment support set up. With these formulations for the radial stresses of the ground, a design of tubing segment support leaves itself would drive through, subject to a verification by measurements. In the following, exemplary analytic formulations are represented for the prognosis of the radial and/or vertical stresses in the roof for the case of an isotropic material behaviour of the rock (Fig. 6(b), Equations (8) - (21)). The developed formulations are presented both for the case of an isotropic material behaviour of the rock and for the case of an anisotropic material behaviour of the rock with consideration of an interface.

The application limits of these formulations are the represented range limits in Table 2. Likewise it is to be noted that the formulations of the ground pressure can be used for the design of the tubing segment support only if the criterion for the risk of blocking the shield skin shows that the regular overcut is sufficiently dimensioned and the rock on the shield skin cannot present itself.

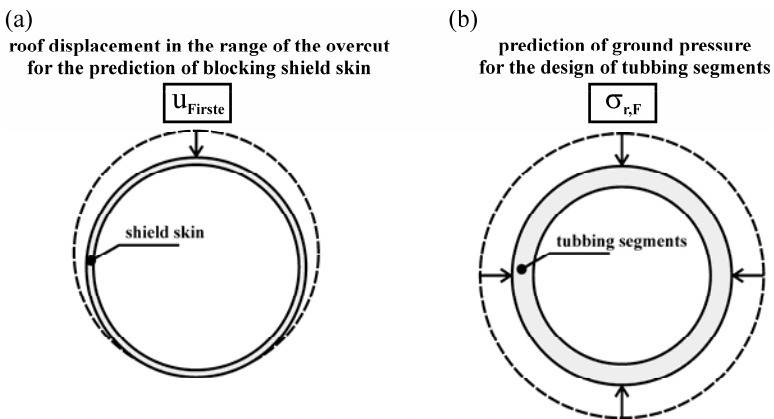


Fig. 6 Overall of view analytical design formulations

Analytical design formulations for the prediction of blocking shield skin u_{Firste} :

$$u_{\text{Firste}} = f_L \times \left(\frac{1000}{E_{\text{Gebirge}}} \times (a \times h_{\text{Ü}}^3 + b \times h_{\text{Ü}}^2 + c \times h_{\text{Ü}}) + d \right) \times \eta_{\text{RK}} \leq 0 \quad (1)$$

$$f_L = 4.7 \times 10^{-2} \times \gamma_{\text{Gebirge}} - 0.228 \quad (2)$$

$$a = \frac{a_E}{c_{\text{Gebirge}} \times a_{\varphi}} \quad (3)$$

$$b = -\frac{14.5}{c_{\text{Gebirge}} \times b_{\varphi}} \times b_M \quad (4)$$

$$c = -\frac{c_E \times c_{\text{Gebirge}}}{c_{\varphi}} - 0.018 \quad (5)$$

$$d = \frac{d_E}{c_{\text{Gebirge}} \times d_{\varphi}} - 0.2 \quad (6)$$

$$\eta_{\text{RK}} = 1.02 \quad (7)$$

with	u_{Firste}	Displacement of roof	[cm]
	γ_{Gebirge}	Unit weight of rock mass	[kN/m ³]
	E_{Gebirge}	E-modulus of rock mass	[MN/m ²]
	c_{Gebirge}	Cohesion of rock mass	[MN/m ²]
	$h_{\text{Ü}}$	Overburden	[m]
	η_{RK}	Safety factor inaccuracy	[-]
		regression functions	
	f_L	Load factor unit weight	[-]

φ_{Gebirge}	15°	20°	25°	30°	35°	40°	≥45°
\mathbf{a}_φ	1.0×10^8	1.5×10^8	1.0×10^9	4.0×10^9	3.0×10^{10}	9.0×10^{10}	1.2×10^{11}
\mathbf{a}_E	-10.0	0.5	4.0	6.0	4.1	0.0	0.0
\mathbf{b}_φ	4.0×10^5	7.0×10^5	1.0×10^6	3.2×10^6	6.2×10^7	1.5×10^8	5.0×10^8
\mathbf{b}_M	3.0	1.5	1.0	1.0	0,9	-1.1	-3.5
\mathbf{c}_φ	7.0×10^2	8.2×10^2	1.0×10^3	1.2×10^3	1.4×10^3	2.0×10^3	3.0×10^3
\mathbf{c}_E	2.0	3.0	3.5	3.5	3.4	3.1	2.9
\mathbf{d}_φ	5.0	7.0	10.0	20.0	30.0	100.0	240.0
\mathbf{d}_E	-3.0	-0.5	1.0	2.0	3.0	4.0	5.0

Table 4 Coefficients

Analytical design formulations for the prediction of radial stresses in the roof $\sigma_{r,F}$:

$$\sigma_{r,F} = f_{L,F} \times f_{TD,F} \times k_F \times \eta_{RK,F} \quad (8)$$

$$f_{L,F} = 4.794 \times 10^{-2} \times \gamma_{\text{Gebirge}} - 0.253 \quad (9)$$

$$f_{TD,F} = 7.114 \times 10^{-3} \times d_T + 0.717 \quad (10)$$

$$k_F = \left(\alpha_F \times h_{\dot{U}}^2 \times a_F + \beta_F \times h_{\dot{U}} \times b_F + \chi_F \times c_F \right) \times mF_{\varphi,c} \quad (11)$$

$$\alpha_F = \frac{-0.00095}{\frac{1000}{E_{\text{Gebirge}}} \times 0.19 + 0.9} \quad (12)$$

$$\beta_F = \frac{-2.23613}{-0.0246 \times \left(\frac{E_{\text{Gebirge}}}{1000} \right)^2 + 0.7102 \times \frac{E_{\text{Gebirge}}}{1000} + 0.3151} \quad (13)$$

$$\chi_F = \frac{57.91231}{0.0961 \times \left(\frac{E_{\text{Gebirge}}}{1000} \right)^2 + 0.489 \times \frac{E_{\text{Gebirge}}}{1000} + 0.56} \quad (14)$$

$$a_F = \frac{1}{\frac{0.085}{c_{\text{Gebirge}}} + 0.9} \quad (15)$$

$$b_F = \frac{1}{0.7252 \times c_{\text{Gebirge}}^2 + 0.7802 \times c_{\text{Gebirge}} + 0.44} \quad (16)$$

$$c_F = \frac{1}{2.6752 \times c_{\text{Gebirge}}^2 + 5.6832 \times c_{\text{Gebirge}} + 1.1407} \quad (17)$$

$$mF_{\varphi,c} = nF_{\varphi} \times c_{\text{Gebirge}} + bF_{\varphi} \quad (18)$$

$$nF_{\varphi} = 0.0026 \times \varphi_{\text{Gebirge}} + 0.182 \quad (19)$$

$$bF_{\varphi} = 1.874757 \times \varphi_{\text{Gebirge}}^{-1.648} \quad (20)$$

$$\eta_{\text{RK},F} = 1.06 \quad (21)$$

with	$\sigma_{r,F}$	Radial stress	[kN/m ²]
	γ_{Gebirge}	Unit weight of rock mass	[kN/m ³]
	E_{Gebirge}	E-modulus of rock mass	[MN/m ²]
	c_{Gebirge}	Cohesion of rock mass	[MN/m ²]
	φ_{Gebirge}	Angle of friction of rock mass	[°]
	$h_{\dot{U}}$	Overburden	[m]
	d_T	Tubbing segment thickness	[cm]
	$\eta_{\text{RK},F}$	Safety factor inaccuracy	[-]
		regression functions	
	$f_{L,F}$	Load factor unit weight	[-]
	$f_{TD,F}$	Load factor tubbing segment thickness	[-]

5 Conclusions

For the analysis of the stress-strain behaviour of rock in mechanical tunnel driving with tubbing segment support extensive numerical studies based on the finite difference method were carried out.

Based on the extensive calculation results of the sensitivity studies several decisive material and geometrical parameters were determined and the development of simple analytical design formulations took place based on regression analyses. On the one hand a criterion was defined by which the risk of blocking the shield skin can be estimated and consequently the size of the necessary regular overcut can be calculated. On the other hand design formulations for the radial stresses of the ground for the rule were found, that is, if the overcut range was sufficient over the entire shield skin length, for the design of the tubing segment support set up. The developed design formulations are presented both for the case of the isotropic material behaviour of the rock and for the case of the anisotropic material behaviour of the rock with consideration of an interface.

The displayed analytical design formulations are based on idealised models and calculation assumptions. The present measured data from realised projects are insufficient to quantifiably verify the calculated radial stresses of the ground with respect to the displacement in the area of the shield. Measurements to verify the analytical design formulations are still pending.

References

Deutscher Ausschuss für unterirdisches Bauen (DAUB) - Ak Schildstatik (2005) Empfehlungen für statische Berechnungen von Schildvortriebsmaschinen, Tunnel 7/2005, S. 44 ff.

DGEG (1980)

Empfehlungen zur Berechnung von Tunneln im Lockergestein (1980) der Deutschen Gesellschaft für Erd- und Grundbau, Taschenbuch für den Tunnelbau 1980, Verlag Glückauf GmbH, Essen

Meißner, H. (1996)

Tunnelbau unter Tage. Empfehlungen des Arbeitskreises 1.6 „Numerik in der Geotechnik“ der Deutschen Gesellschaft für Geotechnik, Abschnitt 2, Geotechnik 19, 1996, S. 99 ff.